



Contents lists available at ScienceDirect

Journal of Photochemistry and Photobiology B: Biology

journal homepage: www.elsevier.com/locate/jphotobiol

Light histories influence the impacts of solar ultraviolet radiation on photosynthesis and growth in a marine diatom, *Skeletonema costatum*

Wanchun Guan^a, Kunshan Gao^{b,*}^aState Key Laboratory of Freshwater Ecology and Biotechnology, Institute of Hydrobiology, Chinese Academy of Sciences, Wuhan, Hubei 430072, China^bState Key Laboratory of Marine Environmental Science, Xiamen University, Xiamen, Fujian 361005, China

ARTICLE INFO

Article history:

Received 11 January 2008

Received in revised form 14 March 2008

Accepted 18 March 2008

Available online xxx

Keywords:

Growth

Photosynthetic rate

Skeletonema costatum

UVR

 Φ_{PSII}

ABSTRACT

Phytoplanktonic species acclimated to high light are known to show less photoinhibition. However, little has been documented on how cells grown under indoor conditions for decades without exposure to UV radiation (UVR, 280–400 nm) would respond differently to solar UVR compared to those *in situ* grown under natural solar radiation. Here, we have shown the comparative photosynthetic and growth responses to solar UVR in an indoor- (IS) and a naturally grown (WS) *Skeletonema costatum* type. In short-term experiment (<1 day), Φ_{PSII} and photosynthetic carbon fixation rate were more inhibited by UVR in the IS than in the WS cells. The rate of UVR-induced damages of PSII was faster and their repair was significantly slower in IS than in WS. Even under changing solar radiation simulated for vertical mixing, solar UVR-induced higher inhibition of photosynthetic rate in IS than in WS cells. During long-term (10 days) exposures to solar radiation, the specific growth rate was much lower in IS than WS at the beginning, then increased 3 days later to reach an equivalent level as that of WS. UVR-induced inhibition of photosynthetic carbon fixation in the IS was identical with that of WS at the end of the long-term exposure. The photosynthetic acclimation was not accompanied with increased contents of UV-absorbing compounds, indicating that repair processes for UVR-induced damages must have been accelerated or upgraded.

© 2008 Elsevier B.V. All rights reserved.

1. Introduction

Solar ultraviolet radiation (UVR, 280–400 nm) is known to affect microalgae and aquatic primary production [1,2]. The deleterious effects of UVR include inhibition of growth and photosynthesis [3–5], damage of proteins and DNA [6–9] and suppression of nutrient uptake [10]. On the other hand, positive effects of UVR have also been documented, such as UV-A-aided repair of damaged DNA [6], UVR-driven photosynthetic carbon fixation in the absence of PAR [11] and UV-A-enhanced photosynthesis in the presence of it [12–15].

Phytoplankton species show different abilities to cope with high levels of PAR and UVR. Cells harvested from deeper layers tend to be more sensitive to high levels of PAR and UVR [16,17], while those in shallow water layers are more resistant to high PAR as well as UVR [14,18]. However, algal species grown under indoor conditions are usually used to explore their eco-physiological responses to UVR [4,5,19].

Indoor-grown species are usually exposed to artificial light sources in the absence of UVR (either in a UV-B-opaque glass vessels or under UVR-free illumination). These species might have

adapted to the UVR-free environment, and can be very sensitive to UVR and high levels of PAR because intensity and quality of irradiation can alter structural and functional features of the photosynthetic apparatus [20]. Consequently, responses to UVR of the indoor-grown cells, especially those grown for decades, may not reflect what happens in nature considering the radiation shock when shifted from indoor to outdoor conditions.

This study aims to investigate photosynthetic response of *Skeletonema costatum*, a cosmopolitan and ecologically important diatom, to solar UV radiation and to examine the difference in photosynthetic performance between the indoor and naturally grown cells while exposing them to constant and changing levels of UVR and PAR.

2. Materials and methods

2.1. Species and culture conditions

Two types of *S. costatum*, an indoor-maintained type (IS) and another isolated from natural seawater (WS), were used for this study. The IS (2042) had been grown under low PAR (<10 $\mu\text{mol photons m}^{-2} \text{s}^{-1}$) for decades and was obtained from the Ocean University of China. The WS was isolated from the coastal water of Nan'ao island (23.47°N, 117.09°E) during July–August,

* Corresponding author. Tel./fax: +86 754 2903977.

E-mail address: ksgao@xmu.edu.cn (K. Gao).

December 2006. It was cultured together with the IS under cool-white fluorescent light of $80 \mu\text{mol photons m}^{-2} \text{s}^{-1}$ (12L:12D) at 25°C in an air-conditioned room for a month before used for experiments. Natural seawater (salinity, 30‰) was sterilized and enriched with f/2 medium [21]. Cells of both IS and WS were inoculated at an initial concentration of $0.5 \times 10^5 \text{ cells ml}^{-1}$ for short or $5 \times 10^5 \text{ cells ml}^{-1}$ for long-term experiments. The uni-algal cultures were carried out with quartz tubes (59 mm in diameter and 350 mm long) which allows equal penetration of PAR and UVR. A water bath with running through seawater was used for temperature control ($24\text{--}25^\circ\text{C}$). All of the cultures were aerated (1 L min^{-1}).

2.2. Experimentation

The experiments were carried out at the Marine Biology Station of Shantou Univ. located in Nan'ao island (23.47°N , 117.09°E) in the South China Sea. Short-term experiments were designed to evaluate effects of solar UVR on photochemical efficiency (Φ_{PSII}) and photosynthetic carbon fixation. Long-term experiments were performed to examine the acclimation of the indoor-grown cells to solar UVR.

2.2.1. Treatments

The cultures in quartz tubes were exposed to three radiation treatments: (1) PAB, tubes covered with a 295 nm cut-off foil (Ultraplan, Digefra, Munich, Germany), transmitting UV-B + A and PAR irradiances above 295 nm; (2) PA, tubes covered with 320 nm cut-off foil (Montagefolie, Folex, Dreieich, Germany), transmitting UV-A and PAR; and (3) P, tubes covered with a 395 nm cut-off foil (Ultraplan UV Opak, Digefra, Munich, Germany), transmitting PAR alone. Triplicate cultures were run under each treatment. The transmission spectra of these foils have been published elsewhere [22].

2.2.2. Short-term experiments

Impact of UVR on the effective quantum yield (Φ_{PSII}) of *S. costatum* was examined during a 60-min exposure (noon time) on July 18th, 2006. Recovery of the yield was followed for 360 min under low PAR ($10 \mu\text{mol photons m}^{-2} \text{s}^{-1}$) provided by a cool-white fluorescent tube. The mean solar irradiances during the 60 min exposure for PAR, UV-A and UV-B were 363.73, 60.98 and 2.01 W m^{-2} , respectively. The biologically weighted UV-B irradiance was 0.20 W m^{-2} (normalized at 300 nm) [23], estimated on the basis of the irradiances reaching the cells in the quartz tubes covered with 295 nm cut-off filter.

In contrast to the above exposures under constant levels of PAR or UVR, the cells were also exposed to changing levels of solar radiation, in a way reflecting their vertical movement during mixing. A device as described in Helbling et al. [14], consisting of 1 fixed (static samples) and 1 rotating system (moving samples), was used. Neutral screens that allowed even attenuation of PAR and UVR were used to obtain 5 levels (100%, 50%, 25%, 13%, 6%) of the irradiances. The turnover rate of the rotating system simulated that of mixing, determining how fast the cells experience the irradiation changes. The static or moving samples were exposed to two radiation treatments, PAR alone or PAR + UVR. The cells in the fixed system (i.e. static samples) received 100% of incident solar radiation during the whole incubation period (1 h). At the beginning of each experiment, three tubes were wrapped in aluminum foil and used as a control for photosynthetic carbon fixation. The turnover time of the wheel, and thus that of the filters in the rotating system, was achieved by using a step motor controlled by a micro-processor. The duration of each rotation (i.e. from 100 to 6 and back to 100% irradiance) varied from 10 to 60 min. Since the experiments lasted 1 h, the number of rotations varied according to the turnover

rate. For example, a turnover time of 10 min, resulted in 6 revolutions. A total of 5 parallel experiments (i.e. fixed and rotating systems) were performed on 5 successive days (noontime, 11:30–12:30) during December 17th to 21th, 2006. The average irradiances during the 1 h incubations were 240.78 (PAR), 36.01 (UV-A) and $0.97 \text{ (UV-B) W m}^{-2}$, respectively.

2.2.3. Long-term experiments

In order to see how the IS acclimates to solar radiation, the cells were cultured semi-continuously (initial and renewed cell density at $5 \times 10^5 \text{ cells ml}^{-1}$), by diluting the culture with fresh medium every 24 h. The cells in quartz tubes were exposed to full spectrum solar radiation for 10 days (from August 17th to 27th, 2006). Cells were counted under microscope (BX50F4, Olympus optical CO. Ltd., Japan) with a haemocytometer. Growth rate was estimated every 24 h, and photosynthetic carbon fixation rate was determined at the beginning (t_0) and end (day 10, t_{10}) of the exposure. Parallel comparisons were made between the IS and WS or among the treatments with or without UV-A or UV-B.

2.3. Measurements and determinations

2.3.1. Quantum yield and photosynthetic carbon fixation

The effective quantum yield (Φ_{PSII}) was measured with a pulse-amplitude-modulated (PAM) fluorometer (PAM-WATER-ED, Walz, Germany), as described previously [5], and calculated according to Genty et al. [24]:

$$\Phi_{\text{PSII}} = \Delta F / F'_m = (F'_m - F_t) / F'_m \quad (1)$$

where the effective quantum yield ($\Delta F / F'_m$) was determined by measuring the instant maximal fluorescence (F'_m) and the steady state fluorescence (F_t) of light-adapted cells.

The rate of UVR-induced damage to photosynthetic apparatus (k , in min^{-1}) and corresponding repair rate were estimated according to previous studies [4,19] as follows:

$$Y_n / Y_0 = r / (r + k) + k / (k + r) * e^{-(k+r)t} \quad (2)$$

where Y_n and Y_0 , respectively, represent Φ_{PSII} values at t_n or t_0 time.

UVR-induced inhibition of Φ_{PSII} was calculated as

$$\text{Inh}(\%) = (Y_p - Y_x) \times Y_p^{-1} \times 100 \quad (3)$$

$$\text{Inhibition per } E_{\text{PAR}} (\text{IPP}) = \text{Inh}(\%) \times E_{\text{PAR}}^{-1} \quad (4)$$

where Y_p indicates the Φ_{PSII} or photosynthetic rate under P treatment, while Y_x indicates that under either PA or PAB treatments. E_{PAR} indicates the mean irradiance of PAR during the incubated period.

2.3.2. Photosynthetic carbon fixation

Samples of 15 ml were inoculated each with $50 \mu\text{l}$ of $5 \mu\text{Ci}$ (0.185 MBq) of labeled sodium bicarbonate (ICN Radiochemicals). After the incubations of 1 h, cells were filtered onto a Whatman GF/F glass fiber filter (25 mm), which was then placed in a 20 ml scintillation vial, exposed to HCl fumes overnight and then dried at 45°C to expel the inorganic ^{14}C . The radioactivity of the fixed ^{14}C was counted with a scintillation counter (LS 6500 Multi-Purpose Scintillation Counter, Beckman Coulter, USA) after the filter was digested in the cocktail (Wallac Optiphase HiSafe 3, Perkin-Elmer life and Analytical Sciences, USA).

2.3.3. Growth rates and pigment determination

The specific growth rate (μ) was determined as follows:

$$\mu = \ln(C_n / C_{n-1}) / (t_n - t_{n-1}) \quad (5)$$

where C_n and C_{n-1} represent the cell concentrations after or before 24 h ($t_n - t_{n-1}$) incubation, respectively.

Chlorophyll-*a* (Chl-*a*) and carotenoids were extracted with 90% acetone and determined from the scanned absorption values using the equation of Strickland and Parsons [25].

2.3.4. Radiation measurement

Incident solar radiation was continuously monitored using a broadband filter radiometer (ELDONET, Real Time Computer Inc., Germany) that has three channels respectively for UV-B (280–315 nm), UV-A (315–400 nm) and PAR (400–700 nm). The radiometer is permanently installed on the roof of Nan'ao (23.47°N, 117.09°E), and measures the irradiances every second and records the mean for each minute into a PC [26]. This instrument has been certificated with having the correspondence error less than 0.5% in comparison with the most accurate instrument (certificate No. 2006/BB14/1). It has been calibrated regularly with the assistance from the maker every year.

2.3.5. Data analysis

A one-way analysis of variance (ANOVA) was used to determine significant difference among the radiation treatments. The significant level was set at 0.05.

3. Results

3.1. Short-term experiments

When the cells of *S. costatum* were exposed to different solar radiation treatments with or without UVR (or UV-B), the effective quantum yield decreased from 0.57 to 0.14 for WS and to 0.03 for IS in 10 min under PAR + UVR (PAB) (Fig. 1 A,B). Removal of UV-B (PA) and UV-B + A (P) resulted in less inhibition of the yield in both WS and IS. In view of the reduction of the yield, PAR led to 63% in WS and 85% in IS, respectively. Presence of UV-A resulted in additional inhibition by 5% in WS and 11% in IS, respectively. Addition of UV-B resulted in further inhibition by 10% and 2% in WS and IS, respectively. As indicated in the Φ_{PSII} ratio of IS to WS (Fig. 1C), Φ_{PSII} decreased much slower in WS than in IS. The rates of repair (r) and damage (k), estimated from the constant levels of Φ_{PSII} under different radiation treatments, were much faster in WS than in IS. Under PAR alone, repair rate was 0.129 for WS, and 0.039 for IS, about 2 times faster in the former than the later. In the presence of UV-A (PA treatment), it was 0.108 for WS, and 0.013 for IS, about 7 times faster in the former than the later; while with both UV-A and B (PAB), it was 0.077 for WS, and 0.005 for IS, about 14 times faster in the former than in the later. In contrast to that of IS, the ratio of $r-k$ in WS was 2.6 times under PAR alone, about 10 times in the presence of UV-A and about 19 times higher with both UV-A and UV-B.

The Φ_{PSII} recovered as a first order exponential function of time ($R^2 \geq 0.92$) when shifted to a low PAR of $10 \mu\text{mol m}^{-2} \text{s}^{-1}$ (Fig. 2). The initial slope (α) of the fitted curves was used as an estimate of the recovery rate of Φ_{PSII} , so a higher α indicates a faster recovery (Table 1). The Φ_{PSII} increased much faster in the WS than in the IS; in 60 min, the yield of WS reached 0.46, while that of the IS recovered to only 0.03. The Φ_{PSII} of the cells previously exposed to both PAR and UVR recovered to 0.46 in WS, but only to 0.16 in IS in 360 min, respectively (Fig. 2). The yield of the cells without previously being exposed to UV-B recovered faster regardless of WS or IS. Those without being exposed to UV-A + B achieved the best recovery of the yield in IS. However, no significant difference was found between the previous PAR and PAR + UV-A treatments in the WS cells. The recovery rate was six times faster in the cells previously exposed to PAR alone and about 24 times faster in those to PAR + UVR, in WS than in IS, respectively.

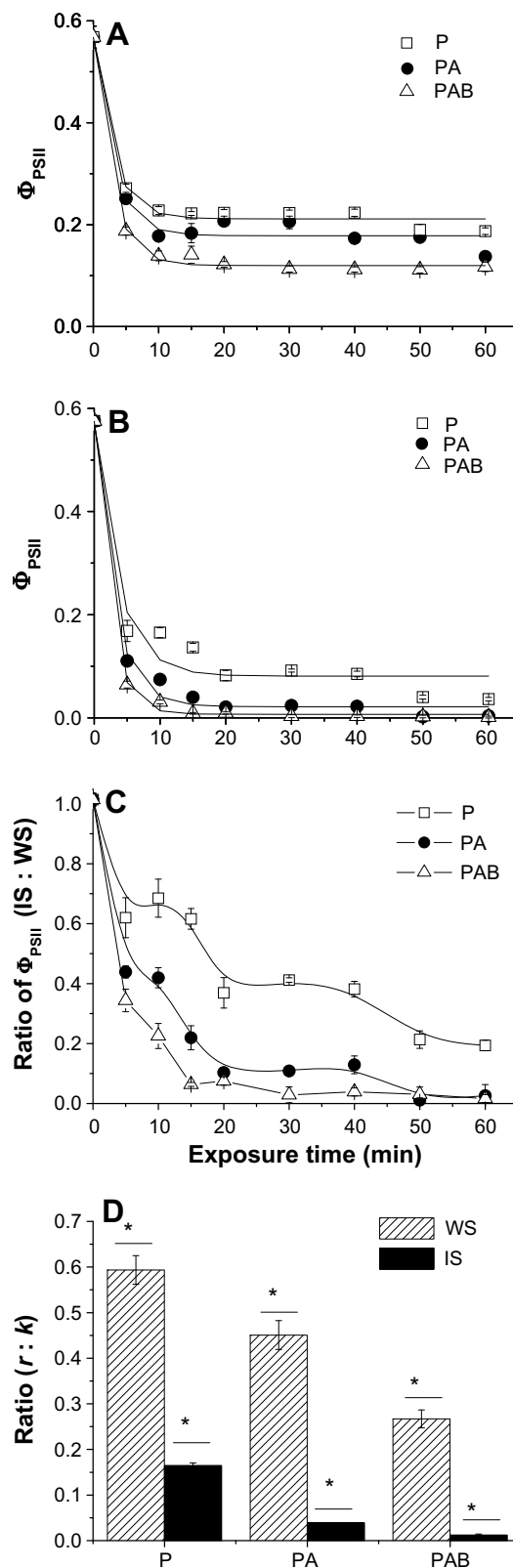


Fig. 1. A, B: Changes in effective quantum yield (Φ_{PSII}) in wild type (WS, A) and indoor-grown stain (IS, B) of *S. costatum* while exposed to solar radiation for 60 min under P (PAR alone), PA (PAR + UV-A) and PAB (PAR + UVR) treatments, respectively; C: the Φ_{PSII} ratio of IS to WS; D: the ratio of repair rate (r , min^{-1}) and damage rate (k , min^{-1}). The vertical bars indicate SD ($n=8$), "*" indicated significant ($p < 0.05$) difference. The mean solar irradiances during 60 min exposure for PAR, UV-A and UV-B was 363.73, 60.98, and 2.01 W m^{-2} , respectively.

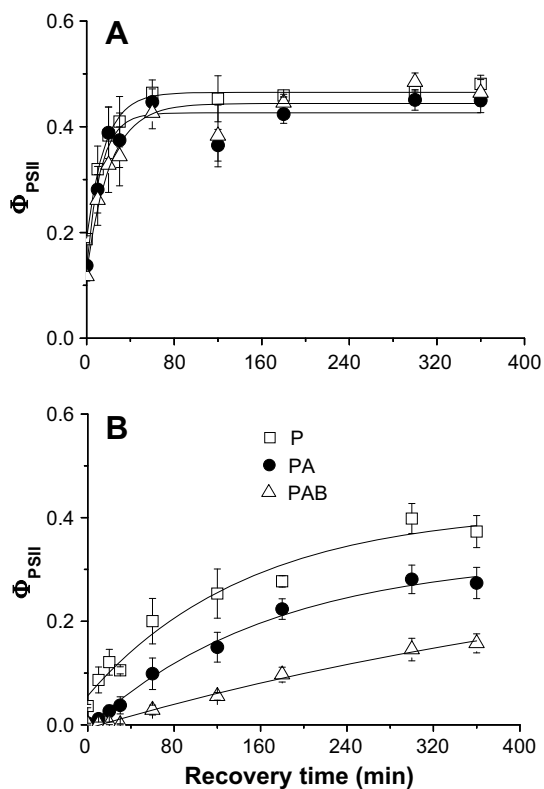


Fig. 2. Recovery of Φ_{PSII} of the wild type (WS, A) and indoor-grown strain (IS, B) of *S. costatum* under the low PAR ($10 \mu\text{mol photons m}^{-2} \text{s}^{-1}$) after the 60 min exposures (conditions as in Fig. 1). The vertical lines indicate SD ($n = 8$). Values were fitted with a first order equation of the form $y = a + b(1 - \exp(-ct))$ ($R^2 \geq 0.92$).

Table 1

Recovery rate (min^{-1}) (the initial change of the yield during the recovery) of the cells under the low PAR level of $10 \mu\text{mol photons m}^{-2} \text{s}^{-1}$ after 60 min exposures to high solar radiation (P, PAR alone; PA, PAR + UV-A; PAB, PAR + UVR)

	P	PA	PAB
WS	0.0148 (0.0007)	0.0148 (0.0010)	0.0128 (0.0005)
IS	0.0021 (0.0003)	0.0018 (0.0002)	0.0005 (0.0002)

SD was shown in parenthesis ($n = 8$).

When the cells were exposed to changing irradiances that reflect their irradiation paths under mixing conditions, their photosynthetic carbon fixation increased with decreased turnover rate (increased circulation time). The non-circulated (static) samples showed depressed photosynthetic rate, especially in the presence of UVR (Fig. 3A). The highest carbon fixation rate was achieved at 60 min per rotation either under PAR or PAR + UVR. The lowest rate was achieved under PAR + UVR for static samples. As indicated in the carbon fixation ratio of IS to WS (Fig. 3B), the photosynthetic rate was much lower in IS than WS under the non-rotated (static) or fast-rotated conditions. The mean percentage difference (inhibition caused by UVR normalized to the mean PAR level during the incubation) indicates that the highest inhibition caused by UVR was observed under the fixed static conditions (Fig. 3C), which was true for both of the cell types. In contrast, changing irradiation (e.g. from 100% to 6%, and back to 100%) during mixing decreased the inhibition. There is no significant difference in the mean percentage difference (inhibition per E_{PAR}) between the two types of the cells when they were irradiated with changing levels of PAR and UVR except at the turnover rate of 30 min when UVR caused higher inhibition of the photosynthesis in IS than WS.

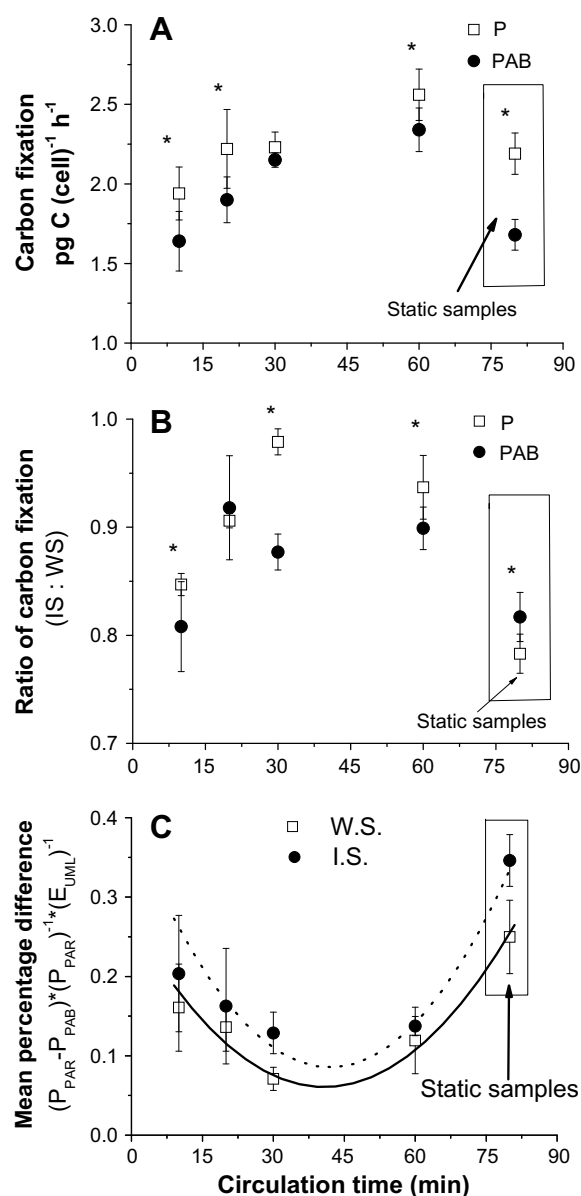


Fig. 3. A: Photosynthetic carbon fixation in wild type (WS) while exposed to changing levels of PAR (P) or PAR + UVR (PAB); B: the carbon fixation ratio of IS to WS as a function of turnover rate; C: the mean percentage difference of UVR-induced inhibition between P and PAB. The vertical bars represent SD ($n = 6$). The mean percentage difference was a function of turnover rate in a two-order equation, $y = c + bx + ax^2$ ($R^2 \geq 0.95$). "*" indicated significant ($p < 0.05$) difference between P and PAB treatment.

3.2. Long-term experiments

During the long-term exposures, the daily dose of solar PAR fluctuated within a range of $2.49\text{--}9.61 \text{ MJ m}^{-2}$, that of UV-A and UV-B within $0.45\text{--}1.54 \text{ MJ m}^{-2}$ and $13.2\text{--}43.1 \text{ kJ m}^{-2}$, respectively (Fig. 4A). The specific growth rate (μ) was much lower in IS than in WS during the initial period of days 1 and 2 (Fig. 4B). It increased obviously at day 3. From day 4, the μ values showed insignificant difference between WS and IS. When the rates of photosynthetic carbon fixation were compared between the two types of the cells at the start (t_0) and end (t_{10}) of the culture (Fig. 5A and B), UVR-induced inhibition of IS was much higher at t_0 but became identical at t_{10} compared with that of WS (Fig. 5C). At the same time, the contents of chl. *a* and carotenoids (pg cell^{-1}) in IS increased and

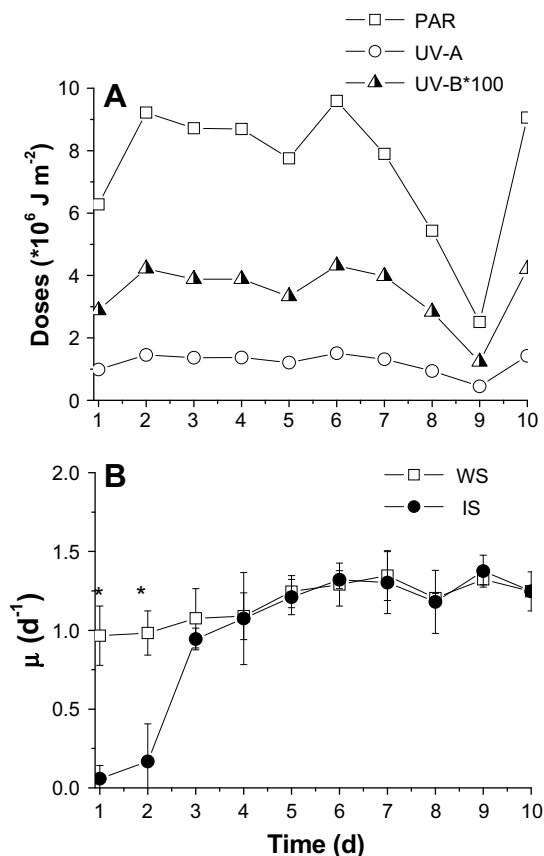


Fig. 4. Daily doses of PAR, UV-A and UV-B (A) and the specific growth rate (μ) (B) of both types of the cells during a long-term culture of 10 days in the presence of UVR. The vertical lines indicate SD ($n = 8$). "*" indicated significant ($p < 0.05$) difference between IS and WS.

was comparative to that of WS as the cells became acclimated to solar radiation (Fig. 6).

4. Discussion

The cells of *S. costatum* grown under indoor conditions for decades, compared with those isolated from natural seawater, were found to be more sensitive to solar UV radiation, with faster damage and slower repair rates of PSII. Such a difference between the two types of the cells reflects the effects of light histories on the cellular defensive strategies against solar UVR. However, the indoor-grown cells had not adapted with genetic modification to the low PAR and UVR-free environment, since they gained the efficiency in coping with UVR during their acclimation to solar UVR.

Slower repair and faster damage rates (Fig. 1) must have led to reduced photosynthetic carbon fixation under static conditions or at the turnover rate of 30 min per rotation (Fig. 3) which either induced higher damage or limited the repair processes. Since the IS cells required longer time to repair the UVR-induced damage (Figs. 1 and 2), their photosynthetic carbon fixation was relative higher at the slower turnover rates (60 min per circulation) (Fig. 3B). Ratio of PAR to UV-B can modulate the effect of UV-B [27]. Cells in the water column are driven up and down with vertical mixing dynamics. The higher recovery rate under low PAR condition (Fig. 2) can reflect the situation when the cells are taken to deep layers after being damaged at the water surface during mixing (Fig. 1). The duration of stay under dim PAR levels at deeper water layers determines the repair of UVR damage of D1 protein and DNA that occurred at surface water. Obviously, vertical mixing rate is critical for the balance between UVR-induced damage and the recovery.

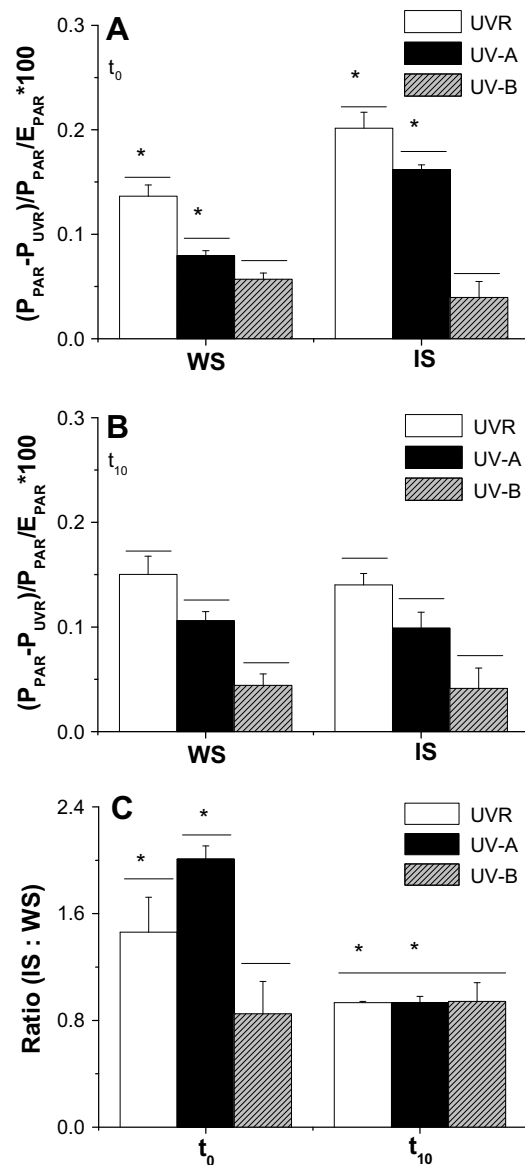


Fig. 5. UVR-induced inhibition of photosynthetic carbon fixation of *S. costatum* at t_0 (A) and t_{10} (B) after normalized to the mean PAR irradiance during the incubations. The inhibition ratio of IS to WS was shown in (C). The vertical lines indicate the SD ($n = 3$). "*" indicated significant ($p < 0.05$) difference.

UVR-induced the lowest inhibition of photosynthetic carbon fixation at the turnover rates between 30 and 60 min per rotation (Fig. 3). This must be related to the maximal repair rate and optimal extent of damage. The faster the turnover rate (in the range of 15–45 min), the less damage caused by UVR, which mirrors less photoinhibition. On the other side, the slower the turnover rate (longer rotations), the higher the UVR-related inhibition, reflecting more damage with elongated exposure at high radiation and inadequate repair. Previous studies showed a linear relationship between the photoinhibition values examined as photosynthetic rate and Φ_{PSII} [8]. In view of the growth rate and UVR-induced photosynthetic inhibition (Figs. 4 and 5), the response of IS cells became identical with those of WS in 3 days during the acclimation. At this point, UVR-caused damages to the cellular components and corresponding repair must be identical between the two types of the cells. The IS cells have achieved the acclimation by adjusting contents of carotenoids (Fig. 6), which play an important role in photoprotection. Adjustment of photosystem (PSI and PSII) size might also have contributed to the acclimation

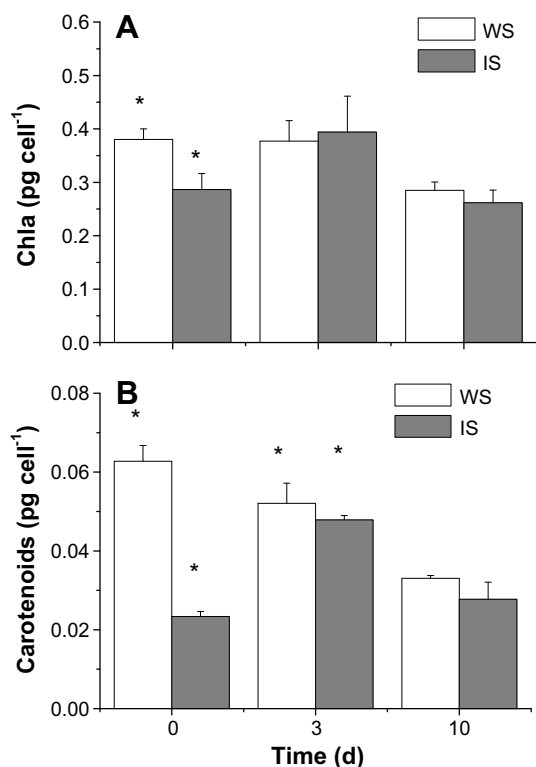


Fig. 6. Contents of Chl. *a* (A) and carotenoids (B) in the WS and IS cells at t_0 , day 3 and day 10 during the acclimation. The vertical lines indicate the SD ($n = 2$), "*" indicated significant ($p < 0.05$) difference between IS and WS.

[28–30]. Accumulation of UV-absorbing compounds, such as mycosporine-like amino acids, is known to be protective against UVR. However, there was no significant increase in these compounds while *S. costatum* cells (4–6 μm) were grown under full spectrum of solar radiation. Usually, small-sized cells are incapable of synthesizing UV-absorbing compounds [31,32].

Different light histories of *S. costatum* resulted in different photosynthetic and growth responses to solar UVR. The acclimating time for this difference to disappear was 3 days for *S. costatum* in the present study, however, it could be species-specific and depends on to what extent the light histories differ. In the present study, the WS cells had been grown under indoor conditions for a month after being isolated from surface seawater, however, its capability to cope with solar UVR sustained when re-exposed to solar radiation. The defensive strategies against UVR in the IS cells must have been down-regulated in a much longer time scale during its indoor-grown history of decades.

Acknowledgements

This study was funded by National Natural Science Foundation of China (Key Project No. 90411018) and Ministry of Education.

References

- [1] J. Beardall, J.A. Raven, The potential effects of global climate change on microalgal photosynthesis, growth and ecology, *Phycologica* 43 (2004) 26–40.
- [2] D.P. Häder, H.D. Kumar, R.C. Smith, R.C. Worrest, Effect of solar UV radiation on aquatic ecosystems and interactions with climate change, *Photochem. Photobiol.* 6 (2007) 267–285.
- [3] E.W. Helbling, V.E. Villafañe, M.E. Ferrario, O. Holm-Hansen, Impact of natural ultraviolet radiation on rates of photosynthesis and on specific marine phytoplankton species, *Mar. Ecol. Prog. Ser.* 80 (1992) 89–100.
- [4] P. Heraud, J. Beardall, Changes in chlorophyll fluorescence during exposure of *Dunaliella tertiolecta* to UV radiation indicate a dynamic interaction between damage and repair processes, *Photosyn. Res.* 63 (2000) 123–134.

- [5] K.S. Gao, W.C. Guan, E.W. Helbling, Effects of solar ultraviolet radiation on photosynthesis of the marine red tide alga *Heterosigma akashiwo* (Raphidophyceae), *J. Photochem. Photobiol. B Biol.* 86 (2007) 140–148.
- [6] D. Karentz, J.E. Clearver, D.L. Mitchell, Cell survival characteristics and molecular responses of Antarctic phytoplankton to ultraviolet-B radiation, *J. Phycol.* 27 (1991) 326–341.
- [7] P. Boelen, M.K. De Boer, G.W. Kraay, M.J.W. Veldhuis, A.G.J. Buma, UV-BR-induced DNA damage in natural marine picoplankton assemblages in the tropical Atlantic Ocean, *Mar. Ecol. Prog. Ser.* 193 (2000) 1–9.
- [8] J. Grzymalski, C. Orrico, O.M. Schofield, Monochromatic ultraviolet light induced damage to Photosystem II efficiency and carbon fixation in the marine diatom *Thalassiosira pseudonana* (3H), *Photosyn. Res.* 68 (2001) 181–192.
- [9] F.S. Xiong, Evidence that UV-B tolerance of the photosynthetic apparatus in microalgae is related to the D1-turnover mediated repair cycle *in vivo*, *J. Plant. Physiol.* 158 (2001) 285–294.
- [10] M.J. Behrenfeld, J.T. Hardy, H. Il. Lee, Ultraviolet-B radiation effects on inorganic nitrogen uptake by natural assemblages of oceanic phytoplankton, *J. Phycol.* 31 (1995) 25–36.
- [11] K.S. Gao, Y.P. Wu, G. Li, H.Y. Wu, V.E. Villafañe, E.W. Helbling, Solar UV radiation drives CO₂ fixation in marine phytoplankton: a double-edged sword, *Plant Physiol.* 144 (2007) 54–59.
- [12] A. Neori, M. Vernet, O. Holm-Hansen, F.T. Haxo, Comparison of chlorophyll far-red and red fluorescence excitation spectra with photosynthetic oxygen action spectra for photosystem II in algae, *Mar. Ecol. Prog. Ser.* 44 (1988) 297–302.
- [13] E.S. Barbieri, V.E. Villafañe, E.W. Helbling, Experimental assessment of UV effects on temperate marine phytoplankton when exposed to variable radiation regimes, *Limnol. Oceanogr.* 47 (2002) 1648–1655.
- [14] E.W. Helbling, K.S. Gao, R.J. Goncalves, H.Y. Wu, V.E. Villafañe, Utilization of solar UV radiation by coastal phytoplankton assemblages off SE China when exposed to fast mixing, *Mar. Ecol. Prog. Ser.* 259 (2003) 59–66.
- [15] C. Mengelt, B.B. Prézelin, UV-A enhancement of carbon fixation and resilience to UV inhibition in the genus *Pseudo-nitzschia* may provide a competitive advantage in high UV surface waters, *Mar. Ecol. Prog. Ser.* 301 (2005) 81–93.
- [16] C. Callieri, G. Morabito, Y. Huot, P.J. Neale, E. Litchman, Photosynthetic response of pico- and nanoplanktonic algae to UV-B, UV-A and PAR in a high mountain lake, *Aquat. Sci.* 63 (2001) 286–293.
- [17] V.E. Villafañe, K.S. Gao, P. Li, G. Li, E.W. Helbling, Vertical mixing within the epilimnion modulates UVR-induced photoinhibition in tropical freshwater phytoplankton from southern China, *Freshwater Biol.* 52 (2007) 1260–1270.
- [18] P.J. Neale, R.F. Davis, J.J. Cullen, Interactive effects of ozone depletion and vertical mixing on photosynthesis of Antarctic phytoplankton, *Nature* 392 (1998) 585–589.
- [19] M.P. Lesser, J.J. Cullen, P.J. Neale, Carbon uptake in a marine diatom during acute exposure to ultraviolet B radiation: relative importance of damage and repair, *J. Phycol.* 30 (1994) 183–192.
- [20] D. Bhaya, R. Schwarz, A.R. Grossman, Molecular responses to environmental stress, in: B.A. Whitton, M. Potts (Eds.), *The Ecology of Cyanobacteria*, Kluwer Academic Publishers, Netherlands, 2000, pp. 397–408.
- [21] R.R.L. Guillard, J.H. Ryther, Studies on marine planktonic diatoms. I. *Cyclotella nana* (Hustedt) and *Detonula confervaceae* (Cleve), *Can. J. Microbiol.* 8 (1962) 229–239.
- [22] F.L. Figueroa, S. Salles, J. Aguilera, C. Jiménez, J. Mercado, B. Viñeola, A. Flores-Moya, M. Altamirano, Effects of solar radiation on photoinhibition and pigmentation in the red alga *Porphyra leucosticta*, *Mar. Ecol. Prog. Ser.* 151 (1997) 81–90.
- [23] R.B. Setlow, The wavelengths in sunlight effective in producing skin cancer: a theoretical analysis, *Proc. Natl. Acad. Sci. USA* 71 (1974) 3363–3366.
- [24] B.E. Genty, J.M. Briantais, N.R. Baker, Relative quantum efficiencies of the two photosystems of leaves in photorespiratory and non-photorespiratory conditions, *Plant Physiol. Bioch.* 28 (1989) 1–10.
- [25] J.D.H. Strickland, T.R. Parsons, *A Practical Handbook of Seawater Analysis, Pigment Analysis*, vol. 167, Bulletin Fisheries Research Board of Canada, 1968, pp. 49–80.
- [26] D.P. Häder, M. Lebert, R. Marangoni, G. Colombetti, ELDONET – European light dosimeter network hardware and software, *J. Photochem. Photobiol. B Biol.* 52 (1999) 51–58.
- [27] K. Shelly, P. Heraud, J. Beardall, Interactive effects of PAR and UV-B radiation on PSII electron transport in the marine alga *Dunaliella tertiolecta* (Chlorophyceae), *J. Phycol.* 39 (2003) 509–512.
- [28] P.G. Falkowski, T.G. Owens, A.C. Ley, D.C. Mauzerall, Effects of growth irradiance levels on the ratio of reaction centres in two species of marine phytoplankton, *Plant Physiol.* 68 (1981) 969–973.
- [29] D. Suggett, E. Le Floc'h, G.N. Harris, N. Leonardos, R.J. Geider, Different strategies of photoacclimation by two strains of *Emiliania huxleyi* (Haptophyta), *J. Phycol.* 43 (2007) 1209–1222.
- [30] G. Johnsen, E. Sakshaug, Biooptical characteristics of PSII and PSI 33 species (13 pigment groups) of marine phytoplankton, and the relevance for pulse-amplitude-modulated and fast-repetition-rate fluorometry, *J. Phycol.* 43 (2007) 1236–1251.
- [31] F. Garcia-Pichel, A model for internal self-shading in planktonic organisms and its implications for the usefulness of ultraviolet sunscreens, *Limnol. Oceanogr.* 39 (1994) 1704–1717.
- [32] V.E. Villafañe, K.S. Gao, E.W. Helbling, Short- and long-term effects of solar ultraviolet radiation on the red alga *Porphyridium cruentum* (S.F. Gray) Nageli, *Photochem. Photobiol. Sci.* 4 (2005) 376–382.